# Mechanical Characterization of Spinal Dura Using a PD-Controlled Biaxial Tensile Tester

ATSUTAKA TAMURA
*Department of Mechanical and Aerospace Engineering, Graduate School of Engineering, Tottori University*
*4-101 Koyama-minami, Tottori 680-8552, Japan*
*a-tamura@tottori-u.ac.jp*

WATARU YANO
*Department of Mechanical Engineering, Graduate School of Sustainability Science, Tottori University*
*4-101 Koyama-minami, Tottori 680-8552, Japan*
*M19J3055X@edu.tottori-u.ac.jp*

DAICHI YOSHIMURA
*Mechanical and Physical Engineering, Tottori University, 4-101 Koyama-minami, Tottori 680-8552, Japan*
*d.y.08040925@gmail.com*

SOICHIRO NISHIKAWA
*Mechanical and Physical Engineering, Tottori University, 4-101 Koyama-minami, Tottori 680-8552, Japan*
*B16T1081C@edu.tottori-u.ac.jp*

In this study, we developed an equi-load biaxial tensile tester and applied it to a series of mechanical tests using specimens obtained from the porcine spinal dura mater. The dural sample exhibited a nonlinear and anisotropic behavior as it was more deformable in the longitudinal direction rather than in the circumferential direction at lower strains, i.e., mechanical response of the longitudinal direction was significantly compliant in the Toe region compared to that of the circumferential direction under 1:1 biaxial stretching. However, we have not observed a significant difference with respect to the resultant strain and Young's modulus between the longitudinal and circumferential directions at higher strains or in the Linear region. Our results also indicated that the upper thoracic region (T1) was relatively compliant compared to the lumbar region (L), where the failure load was almost equal between them, because the dural thickness of T1 was five-fold greater than that of L, i.e., spinal dura mater became stiffer and stronger at further distances from the brain. This shows structural effectiveness and may be preferable to mechanically protect the vulnerable spinal cord from externally applied impact loads.

*Keywords*: spinal dura mater; biaxial stretch; proportional-derivative (PD) control; spinal cord injury (SCI); cerebrospinal fluid (CSF); spontaneous CSF leak.

## 1. Introduction

Traumatic spinal cord injuries (SCIs) frequently develop dural tears and cerebrospinal fluid (CSF) leaks, which occur in 18%–36% of thoracic-lumbar spinal trauma incidents.[1] Spontaneous CSF leak is now recognized as an important and underdiagnosed cause of new onset headaches.[2–3] In traumatic cases involving SCIs, dural tears are mostly developed at the moment of injury. Because CSF supports the brain and spinal cord inside our body *in vivo*, even a nonfatal hole or minor tear developed in the dura mater will lead to a loss of CSF volume, resulting in intracranial hypotension. CSF leaks are not a life-threatening trauma; however, patients' quality of life can be severely damaged and deteriorated by a lasting pain, which will also result in long-term impairment at high societal cost. Currently, it is hypothesized that CSF leaks start at the site at which the dura mater mechanically fails because the dural membrane is the outermost, thickest, and toughest of the meninges surrounding the spinal cord.[4] Thus, characterizing the dura's mechanical properties and understanding its mechanical strength is essential.

The spinal dura mater is a fibrous dual-layer membrane consisting of an outer periosteal layer and an inner meningeal layer.[5] The thin outer layer primarily comprises extracellular collagen fibers with few elastic fibers.[6] The fibers of the dura are not arranged in a parallel direction and do not run in a longitudinal direction but are oriented in concentric laminae around the spinal cord, meaning fibers preferentially run in a circumferential direction. Because the dura mater is subjected to a planar mechanical load *in vivo*, material characterization of the dura should be conducted under the environment of a biaxial stretch rather than that of a uniaxial stretch.

Accurate mechanical characterization of soft biological materials is critical to predict traumatic injuries occurring in traffic accidents and contact sports, because these data are crucial in formulating a constitutive model with a robust set of parameters. However, for incompressible planar tissue such as a membrane-like material, the analysis of mechanical behavior can be complicated by its intrinsic tissue anisotropy, structural heterogeneities, and artificial inelastic changes induced by asymmetric specimen geometry.[7–10]

In the present study, we have developed an equi-load biaxial tensile tester for soft biological materials, which will be useful in characterizing mechanical data of a membranous specimen subjected to large deformation under moderate-to-sub-traumatic loading conditions. As a first step toward fully understanding the mechanism of spontaneous CSF leak, the objective of this study was to investigate mechanical properties of the spinal dura mater.

## 2. Methods

### *Sample preparation*

Fresh porcine spines ($N$ = 6) were harvested immediately after sacrifice at a local abattoir and carried back to the laboratory with ice packs. Square samples of 15 × 15 mm with a mean thickness of 0.090 ± 0.076 mm ($n$ = 18) were cut out of the periosteal layer of dura attached to the spinal canal located on the thoracic and lumbar portions using a surgical scalpel with distinction in the longitudinal and circumferential directions. These dural samples were carefully kept in a physiological saline to avoid dehydration and further stored in a refrigerator at 4°C until the experiment. Special care was taken for the thickness measurement, where a thickness was measured at each lateral side of the undeformed square sample using a thickness gauge (No. 107, Ozaki MFG, Tokyo, Japan) and a unique mean thickness was calculated by averaging four measured values.

***Biaxial tensile tester***

The samples were mounted on a biaxial tensile tester (Fig. 1) integrated with a pair of custom parallel-plate load cells, which have a resolution of 0.5 mN, such that the longitudinal and circumferential directions were in line with each of the biaxial stretching displacements. Two strain gauges (UFLK-1-11, Tokyo Sokki Kenkyujo, Tokyo, Japan) were glued onto each side of the thin stainless steel plates (50 mm long × 10 mm width × 0.2 mm thick) and the full-bridge circuit, i.e., the four active gauge method, was set up. The custom parallel-plate cantilever arms were then attached to each of the four linear motors (XMSG430, Suruga Seiki, Shizuoka, Japan) that controlled the biaxial stretching in the *x*- and *y*-directions. Of these, two arms acted as sensitive force transducers, i.e., channels 1 and 2, and force data were recorded using a commercial data acquisition system (NR-ST04, Keyence, Osaka, Japan) at 1 kHz per channel. Each of the specimens was carefully manipulated to avoid uncontrolled stretching and severe torsion using micrometers attached to the linear motors. Prior to testing, nine vanilla beans were placed onto the specimen's central surface as a marker such that they would define four squares around the sample center, spaced ~1 mm apart from one another. Nominal stress was calculated by dividing the force measured along each axis by an undeformed cross-section area of the dural sample that was defined by the initial thickness and section width. The biaxial stretching tests were performed in a load control mode. Specifically, sixteen hooks, four per each side via two pulleys, were placed along the edges of the specimen ensuring an equal distance between the hooks.

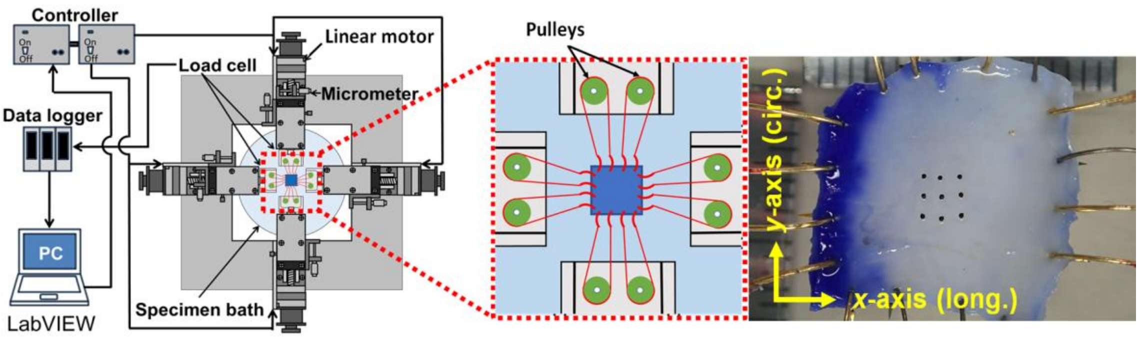


Fig. 1: Schematic of an equi-load biaxial tensile tester. Note that the *x*-axis is aligned with the longitudinal direction of the spinal cord.

Proportional-derivative (PD) control is one of the most widely used algorithms in a closed-loop feedback system. Because the proportional (P) control has a drawback related to the static, or steady state, error, the derivative (D) action is commonly implemented to improve the closed-loop stability,[11–12] i.e., the derivative term is proportional to the time derivative of the control error, allowing an appropriate prediction of future error. Previous studies (see Ref. 13–14) demonstrated that the spinal dura shows a stiffer or stronger mechanical response in the longitudinal direction, rather than its circumferential direction, when subjected to a uniaxial stretch. Thus, a custom PD controller coded in LabVIEW was implemented and equi-load biaxial displacements were imposed on the tethered attachment points at four adjacent sides of the specimen. To realize the PD control in this work, the *x*-axis (longitudinal direction) load was set to slightly precede the *y*-axis (circumferential direction) load, i.e., each of the *x*-axis motors was prescribed to constantly move at a rate of 0.1 mm/s, while the stretching rate of the *y*-axis motors was flexibly varied to precisely track the *x*-axis load (Fig. 2). Notably, the *x*- and *y*-displacements of the paired linear motors were also set to be equal along the two loading axes, and the applied traction forces were almost evenly distributed per side by the four attached tethers.

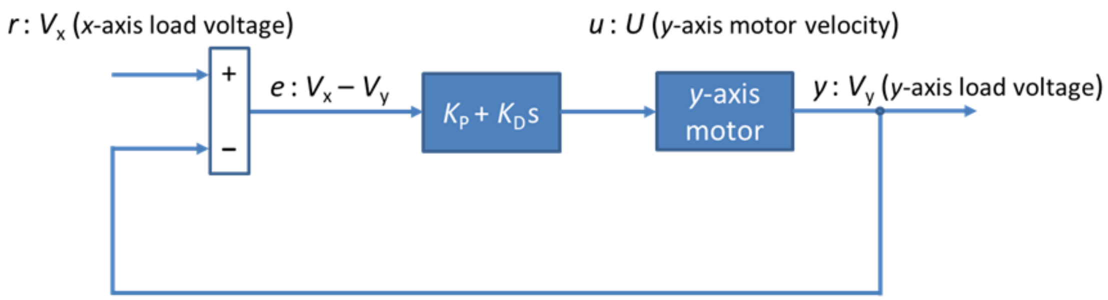


Fig. 2: Schematic diagram of a PD controller implemented for the equi-load biaxial tensile tester. $K_P$ and $K_D$ are controller gains for the proportional (P) and derivative (D) actions. (*x*-axis: longitudinal direction; *y*-axis: circumferential direction)

As shown in Figure 3, all the specimens ($n$ = 18) were mechanically preconditioned by stretching to 6 mm, which was equivalent to ~0.4 N, for four cycles at a constant rate of 0.2 mm/s followed by a 60 s rest. Subsequently, the specimens were preloaded to 0.05 N considering a mechanical creep to define the "zero" point prior to the application of a final stretch. This loading condition was selected to ensure that each specimen was not damaged owing to overstretching and to obtain reproducible and stable mechanical responses. Following the preconditioning cycles and zero point adjustment, an equi-load biaxial stretch was applied until material failure. At the beginning of the final experiment, any specimen that had distinct tears or disruptions at the tether attachment points was discarded, and only eleven specimens ($n$ = 11) were chosen for the subsequent data analysis. The samples were immersed in a physiological saline bath warmed at 37°C with a hot plate (TS-SP, Tokai Hit, Shizuoka, Japan) during the tests. All the experiments were completed within 24 h after swine sacrifice.

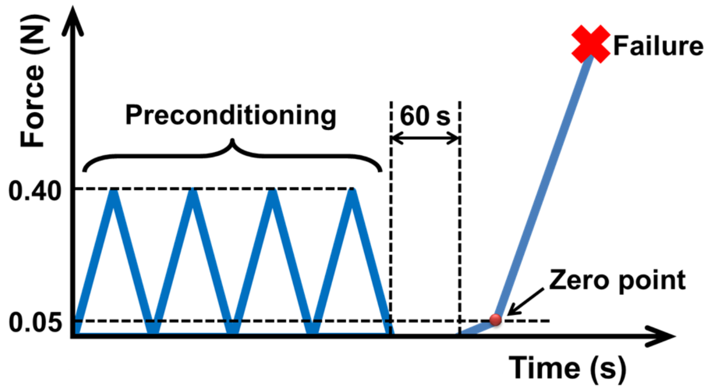


Fig. 3: Protocol of a biaxial tensile test. Four cycles of preconditioning were followed by a 60-s rest, preload setting, and final stretch.

***Data analysis***

To analyze in-plane deformations of the sample during the biaxial stretching test, the displacement of the markers fixed onto the specimen surface was recorded using a digital camera (TG-2, Olympus, Tokyo, Japan) as a movie at 30 fps, which was later subdivided into sequential single images. To synchronize the timing of the measured force data and captured images, an LED light was brought into the field of observation view. When it was manually turned on, the driving voltage of the LED light was also recorded in the data logger (NR-HA08, Keyence, Osaka, Japan). To minimize the potential boundary effects due to trampoline-like grippers, markers inside the central 2 × 2 mm region (~1 mm apart) of the tissue sample were used to calculate the marker displacements. From the measured marker positions, a displacement field within the tracked area was determined and Green-Lagrange strains in normal directions ($E_{11}$ and $E_{22}$) were calculated by performing partial derivatives as given in Eq. (1):

$$E_{\mathrm{IJ}} = \frac{1}{2}\left(\frac{\partial U_{\mathrm{I}}}{\partial X_{\mathrm{J}}} + \frac{\partial U_{\mathrm{J}}}{\partial X_{\mathrm{I}}} + \sum_{\mathrm{K}=1}^{2} \frac{\partial U_{\mathrm{K}}}{\partial X_{\mathrm{I}}}\frac{\partial U_{\mathrm{K}}}{\partial X_{\mathrm{J}}}\right) \quad (1)$$

Herein, $E_{\mathrm{IJ}}$ defines the strains (I, J = 1 or 2), $U_{\mathrm{K}}$ the displacements, and $X_{\mathrm{K}}$ denotes the reference coordinates,[15] i.e., $E_{11}$ and $E_{22}$ are strains in the longitudinal and circumferential directions of the spinal dura mater, which were obtained by averaging those of four squares composed in the specimen's central surface.

A typical load-elongation relation of a membranous soft tissue tested in biaxial stretch shows an exponentially increasing curve, the Toe region, followed by a fairly linear response, the Linear region. Thus, to accurately characterize the material properties of the dura mater, we needed to identify a boundary point between the Toe and Linear regions that was specific to each of the specimens. First, a reference material stiffness, $\alpha$, was calculated based on the gradient of a linear portion obtained for a period of 30 s or more in each of the force-time history curves (Fig. 4). Subsequently, an apparent material stiffness, $\beta$, was similarly computed every 1 s intervals from time zero (0 s) until 30 s, and the boundary point was defined as the timing when $\beta$ exceeded the value of ($\alpha - 0.01$). Finally, Young's moduli of the Toe or Linear regions were calculated for the range between zero and the boundary points or the range between the boundary and failure points, respectively, using custom VBA code (Excel, Microsoft, Redmond, WA, USA) with a least squares method. All statistical analyses were performed using SPSS ver. 24 (IBM, Armonk, NY, USA), where the significant difference was defined as $P < 0.05$.

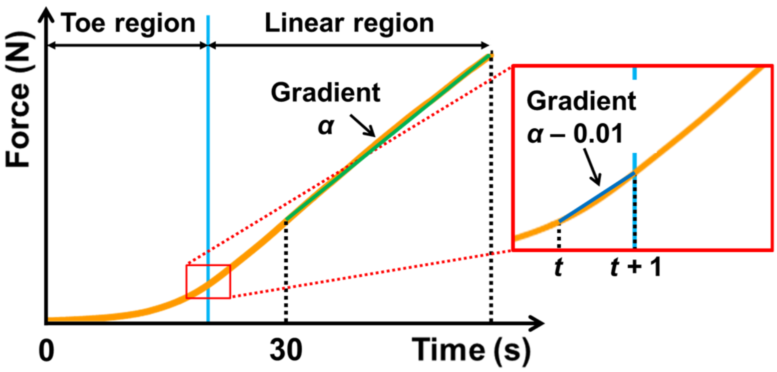


Fig. 4: Definition of a boundary point between the Toe and Linear regions. Gradient $\alpha$ was determined in the Linear region, i.e., time period of 30 s through material failure.

***Histology***

Additional dura mater samples freshly isolated from the upper thoracic (T1) and the lower thoracic (T3) regions as in our previous work (see Ref. 16) were immediately stored and fixed in a 10% phosphate-buffered formalin solution. These membrane-like specimens with a 0.03–0.15 mm thickness were then immunohistochemically-stained using Masson's Trichrome staining and Elastica van Gieson staining protocols to confirm how collagen and elastin fibers were aligned in the dural tissue samples. We used an inverted microscope, (IX73, Olympus, Tokyo, Japan) for bright field observation.

## 3. Results

***Mechanical testing***

When an equi-load biaxial stretch was applied to a specimen, the $x$- and $y$-axes reaction forces increased steadily and almost equivalently (Fig. 5). Most of the specimens failed around 2.4 N, while the resultant strain reached 15%–20% longitudinally and 7%–9% circumferentially. Note that the $x$-axis was set to slightly precede the *y*-axis, while the measured force difference between them consistently fell within the range of 0.06 N during the whole process of the biaxial stretching test. However, in a force–strain curve, the *y*-axis (circumferential) was likely to increase earlier than the *x*-axis (longitudinal), i.e., the *x*-axis was evidently compliant compared to the *y*-axis (Fig. 6). This characteristic strongly depends on an intrinsic material compliance of the longitudinal direction in the lower strains or Toe region, which was significantly indicated ($^{**}P < 0.01$) in Figures 7a and 8a. Conversely, no significant difference was found with respect to material stiffness between the *x*- and *y*-axes in the higher strains or Linear region (Figs. 7b and 8b). Note that the material anisotropy of the dura mater strongly depends on the spinal level. Specifically, the Young's moduli of the lumbar region, L, were significantly higher for the Toe and Linear regions than those of the upper thoracic region, T1 ($^{\ddagger}P < 0.01$). The resultant strain of T1 was also significantly higher than that of L in the Toe region ($^{\dagger}P < 0.05$), providing further support that T1 is more compliant than L in the lower strains.

In the current work, material failure was defined when a distinct tear or damage was detected in the biaxially stretched specimens; the peak load was identified in a force–strain curve at the same timing. On average, peak stress and failure strain of T1 resulted in 1218 ± 419 kPa and 0.202 ± 0.062 (mean ± SD) for the longitudinal direction ($n$ = 5), and 1201 ± 428 kPa and 0.090 ± 0.016 (mean ± SD) for the circumferential direction ($n$ = 5), respectively. Similarly, peak stress and failure strain of L resulted in 6241 ± 2285 kPa and 0.154 ± 0.018 (mean ± SD) for the longitudinal direction ($n$ = 6) and 6058 ± 2134 kPa and 0.068 ± 0.027 (mean ± SD) for the circumferential direction ($n$ = 6), respectively. Of note, only normal (longitudinal and circumferential) forces were measured in this study.

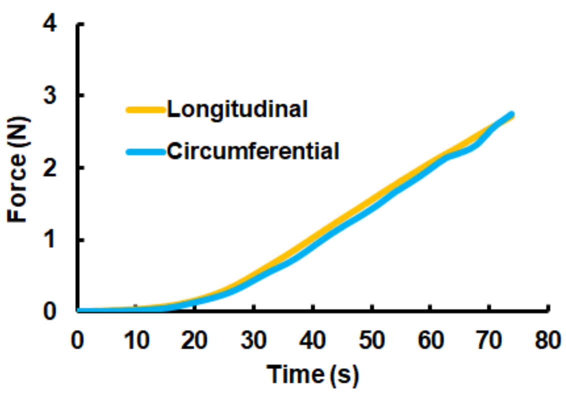


Fig. 5: Typical force-time history during the equi-load biaxial tensile test. The *x*-axis (longitudinal direction) load was set to constantly precede the *y*-axis (circumferential direction) load. The measured force difference between the *x*- and *y*-axes consistently fell within the range of 0.06 N during the test.

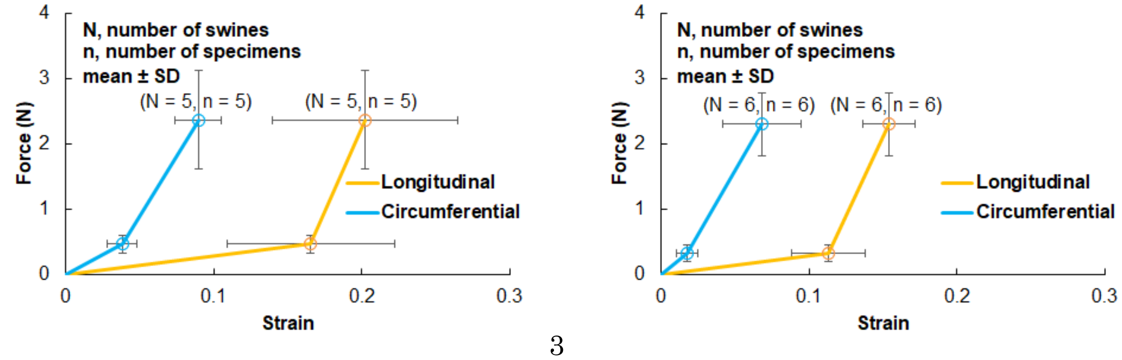


(a) Upper thoracic region (T1).

(b) Lumbar region (L).

Fig. 6: Average force–strain curves obtained for the spinal dura mater subjected to equi-load biaxial stretch (mean ± SD).

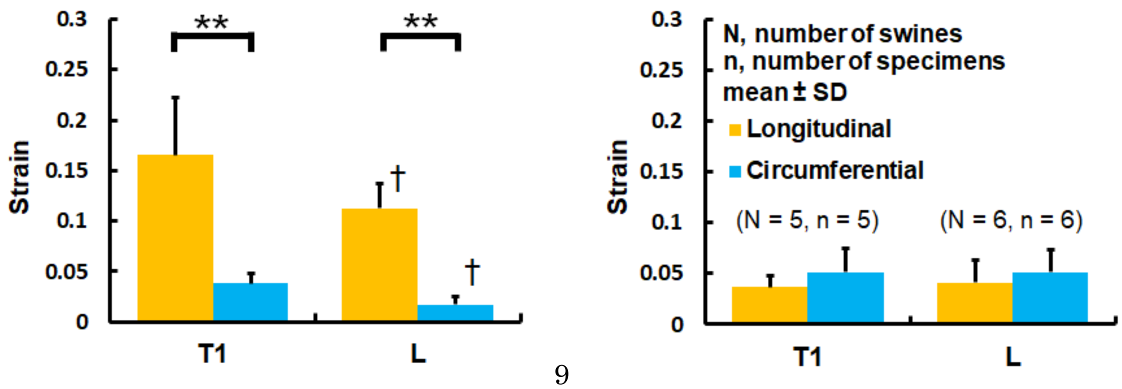


(a) Toe region.

(b) Linear region.

Fig. 7: Comparison of resultant strains of longitudinal and circumferential directions varying with the spinal level ($^{**}P < 0.01$, $^{\dagger}P < 0.05$ vs. T1). T1 and L indicate the upper thoracic and lumbar regions, respectively.

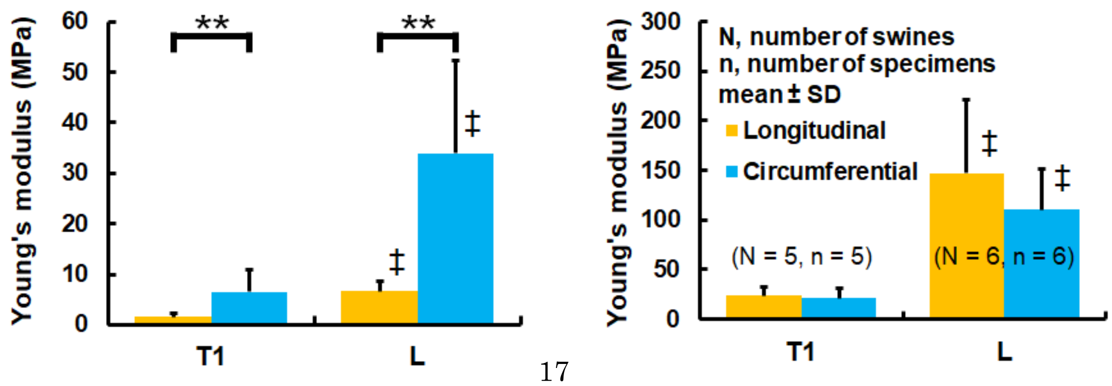


(a) Toe region.

(b) Linear region.

Fig. 8: Comparison of the Young's moduli of the longitudinal and circumferential directions varying with the spinal level ($^{**}P < 0.01$,

‡$P < 0.01$ vs. T1). T1 and L indicate the upper thoracic and lumbar regions, respectively.

***Histology***

Figure 9a demonstrates that collagen fibers were preferably aligned in the circumferential direction in the upper thoracic region (T1) and were randomly aligned in the lower thoracic region (T3). We should also note that many longitudinally undulated wrinkles were observed along the axis of the spinal cord (Fig. 9b), which were seemingly more undulated in T1 rather than T3, suggesting that T1 likely behaves in a more compliant manner compared to T3 when subjected to such a biaxial stretch.

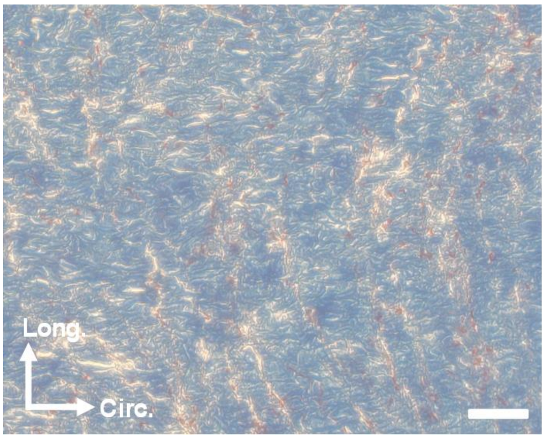


(a) T1 (MT)

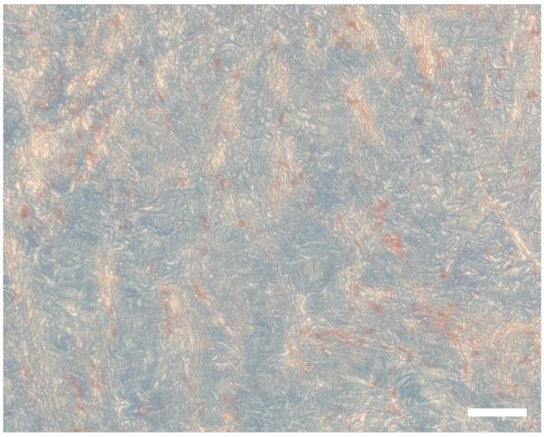

(b) T3 (MT)

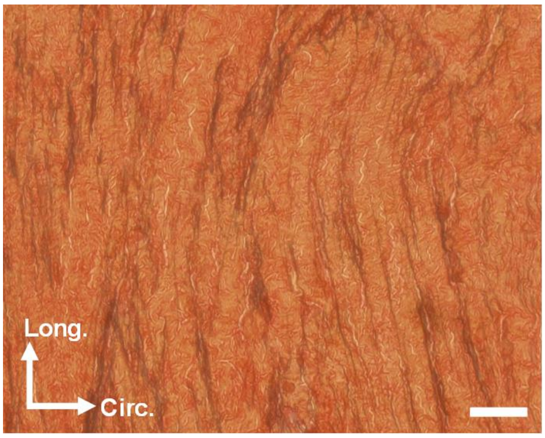


(c) T1 (EVG)

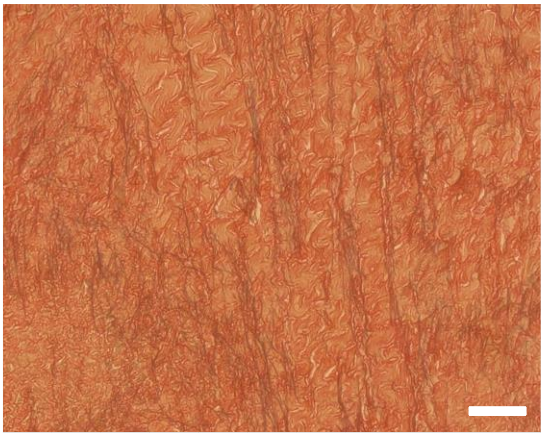

(d) T3 (EVG)

Fig. 9: Immunohistochemically-stained samples obtained from the upper (T1) and lower (T3) thoracic regions (Top: Masson's Trichrome staining, MT; Bottom: Elastica van Gieson staining, EVG), demonstrating that slightly undulated wrinkles were formed along the longitudinal direction. Scale bar is 50 μm (Objective 20×). Long. and Circ. indicate longitudinal and circumferential directions, respectively.

**4. Discussion**

A membrane-like soft biological material is commonly subjected to planar mechanical load *in vivo*. Thus, characterizing mechanical properties of the spinal dura in the loading environment with a biaxial stretch rather than a uniaxial stretch is important. However, considerably limited information is available on the spinal dura mater, because handling such a membranous sample in the biaxial stretching condition is technically difficult. In the present study, we developed an equi-load biaxial tensile tester based on PD control and measured mechanical properties of the porcine periosteal dura specimens obtained from the upper thoracic (T1) and lumbar (L) regions. This load-controlled biaxial tensile tester allowed a square sample to reach a maximum force of ~2.4 N, enabling quantitative comparison of the resultant strains and Young's moduli between the longitudinal and circumferential directions, as well as those related to the spinal level difference. Notably, the equi-load biaxial stretching test was successfully realized in this study within a measurement deviation of 0.06 N between the $x$- and $y$-axes throughout the experiment, as shown in Figure 5.

In the Toe region, T1 was significantly greater than L ($^{\dagger}P < 0.05$) in resultant strain (Fig. 7a), and L (20.2 MPa, $n = 6$) was correspondingly stiffer than T1 (4.0 MPa, $n = 5$) ($^{\ddagger}P < 0.01$) in Young's modulus (Fig. 8a). Nakagawa (1991) investigated the amount of elastin contained in the dura mater along the length of a human spine and found that the ratio of elastin contained in the dorsal side (13.0%) was higher than that contained in the ventral side (7.1%) of the spinal dura.[17] The average ratio of elastin contained in the dura mater was independent of the anatomical sites among the cervical, thoracic, and lumbar regions. This suggests that the total amount of elastin contained in the specimen strongly depends on the thickness of the spinal dura. In the current work, it was revealed that T1 was five-fold greater than L in thickness, meaning the total amount of elastin contained in T1 was much greater than that contained in L. Because T1 is a specific region requiring structural flexibility, it is reasonable to assume that T1 is inherently more compliant than L in the lower strains or Toe region.

As for the Linear region, the resultant strains were comparatively smaller in the longitudinal direction and greater in the circumferential direction in comparison with those of the Toe region, while relatively similar in their magnitude between T1 and L (Fig. 7b). Conversely, the Young's modulus of L (128.7 MPa, $n = 6$) was significantly higher than T1 (22.5 MPa, $n = 5$) ($^{\ddagger}P < 0.01$) (Fig. 8b). The reason of this contradiction is currently unknown, but this is probably because the collagen fibers embedded in the tissue from L were relatively taut and abundant compared to those from T1, which would work dominantly in the deformation of the Linear region. As mentioned above, it is interesting to note that T1 (~0.171 mm thick) was significantly thicker than L (~0.030 mm thick), which may have compensated the difference in material stiffness between them, and consequently, the peak load resulted in the same order of magnitude, whereas L was significantly greater than T1 in peak stress (Fig. 10). This may indicate that the spinal dura cannot be regarded as a homogeneous structure along the whole length of the spinal cord. Furthermore, the mechanical compliance of the spinal dura in the longitudinal direction, particularly in the Toe region, implies its inherent high flexibility against flexion or extension of the spine, which may prevent it from breaking during our physiological activity. That is, the initial longitudinal compliance observed in the lower strains or Toe region is structurally protecting the spinal cord. We should also note that Young's moduli obtained in the study were comparable to values reported in previous studies. Specifically, the Young's moduli measured in the Toe and Linear regions mostly fell within the range of 10–150 MPa.[13]

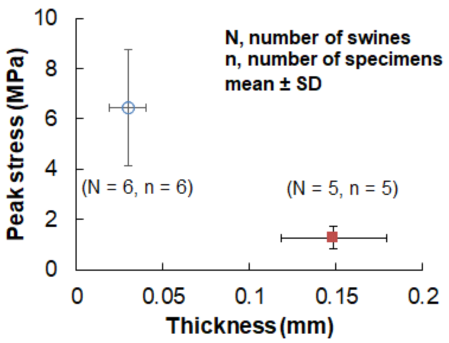


(a) Peak stress vs. thickness.

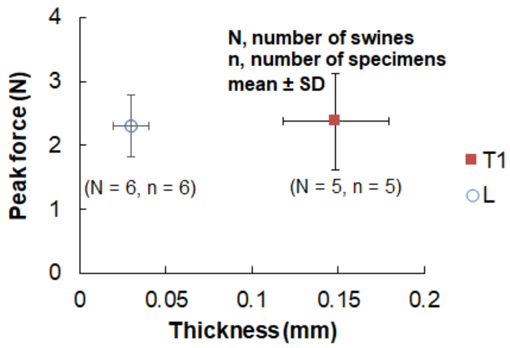


(b) Peak force vs. thickness.

Fig. 10: Peak stress and peak force at failure represented as a function of dural thickness varying with the spinal level. T1 and L indicate the upper thoracic and lumbar regions, respectively.

Runza et al. (1999) investigated human lumbar dura via uniaxially stretching and reported that spinal dura fibers oriented axially. Maikos et al. (2008) also found that spinal dura fibers appeared to be aligning longitudinally in the rat spinal dura mater.[18] Conversely, Persson et al. (2010) performed uniaxial stretching tests and concluded that fibers are randomly aligned in the bovine spinal dura mater.[14] At this moment, there is no consensus on the fiber orientation angle in the spinal dura. However, in the current work, it seems that the immunohistochemically-stained microfibrils were predominantly aligned in the circumferential direction with a little slack (Fig. 9), suggesting that the $y$-axis (circumferential direction) load is likely to increase earlier than the $x$-axis (longitudinal direction) load in force–strain curves when biaxial stretching is applied (Fig. 6). This is consistent with the experimental results obtained by a displacement-controlled biaxial stretch using ovine cervical dura mater samples.[9]

In particular, the longitudinal direction was more significantly compliant than the circumferential direction ($^{**}P < 0.01$) in the lower strains or Toe region (Figs. 7a and 8a). Interestingly, however, no significant difference was found in mechanical response between the longitudinal and circumferential directions in the higher strains or Linear region (Figs. 7b and 8b). As seen in the aortic medial wall mainly composed of smooth muscle layers (SMLs) and elastin layers (ELs), the circumferentially aligned ELs show structural buckling at a unloaded state when the aortic tissue is extracted from the body,[19–20] while SMLs and ELs show a *Baumkuchen*-like, alternately layered, structure at a physiological condition. It was also demonstrated that the longitudinal EL undulation *in vitro* can be numerically reconstructed by superposing a series of circumferential EL waviness along the aortic axis.[21] Thus, for the longitudinal "wrinkle" formation mechanism, which is similarly induced by the superposition of circumferentially-crimped fibers, the greater longitudinal strain observed in the Toe region could be partly ascribed to the undulated wrinkles longitudinally formed in the spinal dura *in vitro*. This can be understood as the initial compliance seen in the longitudinal direction was a dissipation of the undulated wrinkles in response to the applied incremental stretch. Nevertheless, the averaged longitudinal undulations were found to be 1.03 for T1 and 1.02 for T3, respectively, which were calculated as the ratio of undulated length to straight length between both ends of the longitudinal wrinkles. A total of 8 and 5 undulated wrinkles were selected for T1 and T3, respectively, in the trial to calculate the ratios. Notably, Persson et al. (2010) reported that the ratios of crimped fibers to the straight length connecting both ends aligned in the longitudinal and circumferential directions were 1.40 and 1.21, respectively,[14] suggesting that the dura is likely to be elongated in the longitudinal direction. Hence, the initial deformability of the longitudinal dura observed in this study might be attributable to the crimped fibers rather than the undulated wrinkles.

To the authors' knowledge, this is the first study to apply an equi-load biaxial stretch to the dura mater samples. Nevertheless, there are a few limitations to be addressed. The first limitation is the definition of zero point. We defined "zero" force using the mechanical creep of a specimen, and the final ramp displacements were applied after the *x*- and *y*-axes loads were stably maintained at 0.05 N as a preload. However, according to our preliminary study, we found that 0.01 N was too small to eliminate an initial slack in the attached tethers, whereas a 0.05 N preload might be slightly too much, and ~0.03 N would be preferred as a zero point or preload in a future work. The second limitation is the effect of shear deformation. We placed each of the markers ~1 mm apart with a special caution and carefully gripped each of the specimens to minimize the effect of shear deformation. In a previous study,[22] homogeneous stress/strain distribution was observed within 16% of the center region in specimens biaxially tested using suture attachments. It was also shown that the small central tracking area, 14% of the stretched area, would be acceptable to neglect the effects of shear deformation.[23] In this study, the tracking area was approximately 7%, which was small enough to ensure measurement accuracy. Nevertheless, even in such an equi-load biaxial stretch, shear deformation was unavoidable. Thus, we also calculated shear strain, $E_{12}$, and found that maximum $E_{12}$ was approximately 30% of the normal strains, $E_{11}$ and $E_{22}$, obtained at failure. In view of the strength of materials, if we assumed material isotropy of an incompressible specimen, shear stress would be about one order of magnitude lower than the normal stresses, at most. Although the detailed mechanical properties related to shear deformation on porcine spinal dura are not available at present, an instantaneous shear modulus was estimated at 1.20 MPa in the rat spinal dura mater.[18] If this is the case for swine, the maximum shear stress would be much less than 10% of the normal stresses, and the effect of shear deformation would be negligible as well. The third limitation is the limited number of specimens tested herein. Because the available number of swines and specimens, five or six, were still too small, additional tests will be required to enhance the reliability of our test results. As Nakagawa (1991) already pointed out,[17] we should also distinguish specimens from the ventral and dorsal sides because the amount of elastin contained in the dura specimens depends on such an anatomical difference. Because the spinal cord runs along the posterior side of the spine, it is likely that the dorsal and ventral spinal dura is subjected to mechanical stretching in a different manner during our daily activity; the ventral or dorsal sides of the dura are constantly exposed to mechanical stretch during spinal extension or flexion, respectively, which may also strongly affect the resultant elasticity in its mechanical responses.

In conclusion, we developed an equi-load biaxial tensile tester and applied it to a series of mechanical tests using the porcine spinal dura mater. We found that the dura sample shows a nonlinear and material anisotropic behavior with the longitudinal direction being more deformable, i.e., the mechanical response of the longitudinal direction was apparently compliant compared to that of the circumferential direction under 1:1 biaxial stretching. We also found that the upper thoracic region (T1) was relatively compliant compared to the lumbar region (L), while the failure load between them was almost equal, because the thickness of T1 was five-fold greater than that of L, i.e., spinal dura mater became stiffer and stronger with increasing distance from the brain. This would be structurally effective and preferable to mechanically protect the spinal cord.

## Acknowledgments

The authors deeply thank Dr. Jun-ichi Hongu and Mr. Tomohiro Tsukuda, Tottori University, for their useful advice and technical assistance on the development of a PD controller. This study was supported in part by JSPS KAKENHI 19K12782 and AMED-CREST JP19gm0810005h0405.

## References

1. Lee SE, Chung CK, Jahng T-A, Kim CH, Dural tear and resultant cerebrospinal fluid leaks after cervical spinal trauma, *Eur Spine J* **23**: 1772–1776, 2014.
2. Morki B, Spontaneous low pressure, low CSF volume headaches: spontaneous CSF leaks, *Headache* **53**: 1034–1053, 2013.
3. Spears RC, Low-pressure/spinal fluid leak headache, *Curr Pain Headache Rep* **18**: 425, 2014.
4. King AI, *The Biomechanics of Impact Injury: Biomechanical Response, Mechanisms of Injury, Human Tolerance and Simulation*, Springer, 2017.
5. Waldman SD, Pain Review 1st Edition, Saunders, 2009.
6. Watson C, Paxinos G, Kayalioglu G (eds.), The Spinal Cord, Academic Press, 2008.
7. Sacks MS, A method for planar biaxial mechanical testing that includes in-plane shear, *J Biomech Eng* **121**: 551–555, 1999.

8. Perez BC, Tang J, Morris HJ, Palko JR, Pan X, Hart RT, Liu J, Biaxial mechanical testing of posterior sclera using high-resolution ultrasound speckle tracking for strain measurements, *J Biomech* **47**: 1151–1156, 2014.
9. Shetye SS, Deault MM, Puttlitz CM, Biaxial response of ovine spinal cord dura mater, *J Mech Behav Biomed Mater.* **34**: 146–153, 2014.
10. Sommer G, Haspinger DC, Andrä M, Sacherer M, Viertler C, Regitnig P, Holzapfel GA, Quantification of shear deformations and corresponding stresses in the biaxially tested human myocardium, *Ann Biomed Eng* **43**: 2334–2348, 2015.
11. Åström K, Hägglund T, PID Controllers: Theory, Design, and Tuning 2nd Edition, Instrument Society of America, 1995.
12. Hirata M, Control System Design: Getting Started with Arduino and MATLAB, TechShare Inc., 2016.
13. Runza M, Pietrabissa R, Mantero S, Albani A, Quaglini V, Contro R, Lumbar dura mater biomechanics: experimental characterization and scanning electron microscopy observations, *Anesth Analg* **88**: 1317–1321, 1999.
14. Persson C, Evans S, Marsh R, Summers JL, Hall RM, Poisson's ratio and strain rate dependency of the constitutive behavior of spinal dura mater, *Ann Biomed Eng.* **38**: 975–983, 2010.
15. Fung YC, *Biomechanics: Mechanical Properties of Living Tissues* 2nd Edition, Springer, 1993.
16. Tamura A, Sakaya M, Dynamic tensile behavior of fiber bundles isolated from spinal nerve roots: effects of anatomical site and loading rate on mechanical strength, *J Medical Diagnostics* **1**: 031001-031001-6, 2018.
17. Nakagawa H, A morphological and biochemical study of elastin in the human posterior longitudinal ligament and the spinal dura mater, Kawasaki Igakkai Shi Liberal Arts & Sciences **17**: 47–59, 1991 (*in Japanese*).
18. Maikos JT, Elias RAI, Shreiber DI, Mechanical properties of dura mater from the rat brain and spinal cord, Journal of Neurotrauma **25**: 38–51, 2008.
19. Matsumoto T, Goto T, Furukawa T, Sato M, Residual stress and strain in the lamellar unit of the porcine aorta: experiment and analysis, *J Biomech* **37**: 807–815, 2004.
20. Tamura A, Kato Y, Reproduction of kinematic behavior of elastic lamellae in the thoracic aortic media, *Proc. ASME 2018 International Mechanical Engineering Congress and Exposition*, Pittsburgh, PA, USA, Paper No. IMECE2018-87242.
21. Tamura A, Kato Y, Modeling prestress-driven buckling behavior of elastic lamina in the aortic media, *Proc. ASME 2019 International Mechanical Engineering Congress and Exposition*, Salt Lake City, UT, USA, Paper No. IMECE2019-10530 (in press).
22. Sun W, Sacks MS, Scott MJ, Effects of boundary conditions on the estimation of the planar biaxial mechanical properties of soft tissues, *J Biomech Eng* **127**:709–715, 2005.
23. Morales-Orcajo E, Siebert T, Böl M, Location-dependent correlation between tissue structure and the mechanical behavior of the urinary bladder, *Acta Biomaterialia* **75**: 263–278, 2018.